The N-Terminal Tails of the H2A−H2B Histones Affect Dimer Structure and Stability†

Brandon J. Placek and Lisa M. Gloss*

School of Molecular Biosciences, Washington State University, Pullman, Washington 99164-4660

Received June 10, 2002; Revised Manuscript Received September 27, 2002

ABSTRACT: The histone proteins of the core nucleosome are highly basic and form heterodimers in a "handshake motif." The N-terminal tails of the histones extend beyond the canonical histone fold of the hand-shake motif and are the sites of posttranslational modifications, including lysine acetylations and serine phosphorylations, which influence chromatin structure and activity as well as alter the charge state of the tails. However, it is not well understood if these modifications are signals for recruitment of other cellular factors or if the removal of net positive charge from the N-terminal tail plays a role in the overall structure of chromatin. To elucidate the effects of the N-terminal tails on the structure and stability of histones, the highly charged N-terminal tails were truncated from the H2A and H2B histones. Three mutant dimers were studied: ΔN-H2A/WT H2B; WT H2A/ΔN-H2B, and ΔN-H2A/ΔN-H2B. The CD spectra, stabilities to urea-denaturation, and the salt-dependent stabilization of the three truncated dimers were compared with those of the wild-type dimer. The data support four conclusions regarding the effects of the N-terminal tails of H2A and H2B: (1) Removal of the N-terminal tails of H2A and H2B enhance the helical structure of the mutant heterodimers. (2) Relative to the full-length WT heterodimer, the ΔN-H2A/WT H2B dimer is destabilized, while the WT H2A/ΔN-H2B and ΔN-H2A/ΔN-H2B dimers are slightly stabilized. (3) The truncated dimers exhibit decreased *m* values, relative to the WT dimer, supporting the hypothesis that the N-terminal tails in the isolated dimer adopt a collapsed structure. (4) Electrostatic repulsion in the N-terminal tails decreases the stability of the H2A−H2B dimer.

The basic packaging unit of DNA in eukaryotic chromatin is the core nucleosome. This structure contains eight histone proteins, two dimers of H2A−H2B that serve as molecular caps for the central $(H3-H4)_2$ tetramer. Approximately 160 basepairs of DNA are wrapped around the surface of this protein octamer. The nucleosome is no longer considered a simple, static packaging system; rather, the nucleosome is a dynamic regulator of the DNA chemistries in the nucleus, including transcription, replication and repair (*1*, *2*). Several posttranslational modifications of the core histone oligomers are important modulators of the accessibility of DNA in the nucleosome (*3*, *4*). The effects of these modifications are being elucidated as to their "downstream consequences" such as activating transcription or enhancing binding of factors to DNA (for example, ref *5*). However, much less is known about the molecular details of the structural and thermodynamic effects of the posttranslational modifications of the histone proteins. Biophysical characterization of the stability of the core histones and any alterations caused by posttranslational modifications will begin to address such molecular details. In this study, we focus on the N-terminal tails of the H2A−H2B dimer.

The interface of the H2A−H2B dimer is comprised of the "histone fold motif" common to all of the core histones (*6*, *7*) and many other oligomers involved in DNA−protein complexes, such as some of the TAF's (TATA-binding protein-associated factors) (*8*, *9*) (Figure 1). The dimerization of two monomers involves some intertwining of the six helices of the histone fold with association in a head-to-tail manner, termed the "handshake motif" (*10*).

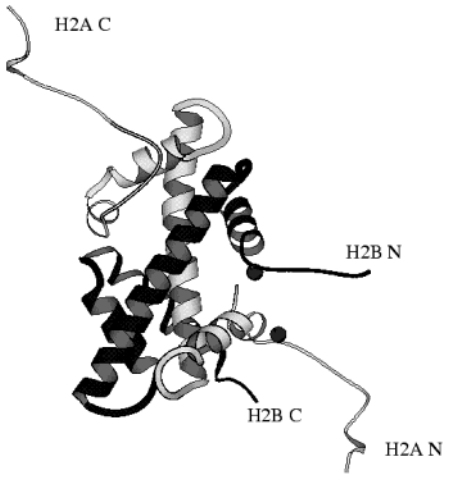

FIGURE 1: Ribbon diagram of the H2A−H2B dimer, derived from the X-ray crystal structure of the core nucleosome (*7*). The H2A monomer is shown as the lighter colored chain. The α-helices of the histone fold motif are represented as wider ribbons. The H2A ribbon includes residues 4−118 (of 129 residues) and that of H2B includes residues 24−122 (of 122 residues). Residue 16 of H2A and residue 32 of H2B are the residues after the N-terminal methionine residue in the ΔN-H2A and ΔN-H2B constructs, respectively; the α-carbons of these residues are denoted by a sphere. The figure was rendered using Molscript v2.1 (*32*).

† This work was supported by grants to L.M.G. from the American Cancer Society (RPG-00-085-01-GMC) and the National Science Foundation (MCB-9983831). B.J.P. was partially supported by a NIH Biotechnology training grant (GM08336-13).

* Corresponding author. Phone: (509) 335-5859. E-mail: lmgloss@wsu.edu.

10.1021/bi026283k CCC: $22.00
Published on Web 11/19/2002

The eukaryotic core histones contain regions of polypeptide N-terminal to the central, globular helical histone fold. The N-terminal tails of the histones are the sites of the regulatory post-translational modifications, and are the most basic regions of the histones. For example, for the *Xenopus laevis* proteins studied here, the histone fold motifs contain an excess of 7 and 5 mol % basic residues for H2A and H2B, respectively. The tails contain no acidic residues, and are 38 and 45 mol % basic residues, for H2A and H2B, respectively. The modifications of the N-terminal tails include acetylation of lysine side chains and methylation of lysine and arginine side chains; acetylation converts a positively charged amine to an uncharged amide, while methylation maintains the positive charge of the modified amino acid. Serine residues in the tails are also sites for phosphorylation, a modification that, like acetylation, alters the charge state of the N-terminal tails. Given that acetylation and phosphorylation decrease the net positive charge of the histones, it is important to determine if electrostatic interactions in the N-terminal tails of H2A and H2B affect the overall stability and structure of the dimer.

To address this question, we measured the urea-induced equilibrium unfolding of three heterodimeric variants of H2A−H2B with N-terminal tail truncations: ΔN-H2A/WT H2B[1]; WT H2A/ΔN-H2B; and ΔN-H2A/ΔN-H2B. The stabilities of these three dimers are compared to the WT H2A−H2B dimer in low salt conditions and as a function of three salts, KCl, KI, and KPi. Similar studies have recently been published on the thermal denaturation of trypsin-treated H2A−H2B dimers (*11*). The work presented here has two major differences from this recent study: (1) By the use of site-directed mutagenesis on the histone genes to generate recombinant truncated H2A and H2B variants, we can differentiate between the effects of the H2A and H2B N-terminal tails. (2) By using different salts, we can determine the mechanism(s) by which salt stabilizes the H2A−H2B dimer.

MATERIALS AND METHODS

Materials. Ultrapure urea was purchased from ICN Biomedicals (Costa Mesa, CA). CM-Sepharose resin was purchased from Sigma (St. Louis, MO); Sephacryl S-100 and Heparin resins were purchased from Amersham Pharmacia (Uppsala, Sweden). All other chemicals were of reagent or molecular biology grade.

Methods. Site-directed mutagenesis was performed on the T_7pET vectors containing the *Xenopus laevis* genes that have been described elsewhere (*12*). Truncations of the codons for the N-terminal sequences of the H2A and H2B genes were performed using extra-long PCR (*13*). Codons for residues 2−15 and residues 2−31 of H2A and H2B, respectively, were deleted from the appropriate genes. The desired truncations and lack of other, undesired mutations in the H2A and H2B genes were confirmed by sequencing the genes in the T_7pET expression plasmids.

Recombinant WT and truncated H2A and H2B histones were overexpressed in *E. coli*, purified, and reconstituted into folded dimers as described in the preceding paper (Gloss and Placek). The homogeneity of the dimeric state of the reconstituted H2A−H2B dimers were confirmed by HPLC size-exclusion chromatography coupled to a static light scattering detector (Dawn EOS from Wyatt Technologies, Santa Barbara, CA).

Data Collection and Analyses. All of the equilibrium unfolding experiments were performed at 25 °C in a buffer of 20 mM potassium phosphate, pH 7.2, with 0.1 mM EDTA. The details of the equipment and data collection methods are reported in the preceding manuscript (Gloss and Placek). The equilibrium urea-induced unfolding transitions were fitted to a dimeric two-state model, using the global data analysis program, Savuka 5.1; the reported errors represent one standard deviation as determined from rigorous analyses of the error surfaces (see Gloss and Placek, preceding paper).

The secondary structural content of the proteins were estimated from the far-UV CD spectra using the CDPro package (*14*). Results were compared from two algorithms: Selcon3 (*15*, *16*) and Contin/ll (*17*, *18*).

RESULTS

Design of the Truncated H2A and H2B Variants. The regions to be truncated in the variants employed in this report were determined from inspection of the X-ray crystal structure of the nucleosome (*7*). N-terminal residues in an extended conformation or unresolved in the X-ray structure were truncated in the variants. The putative N-caps of the N-terminal helices (Thr 16 of H2A and Ser 33 of H2B), as well as the potentially stabilizing carboxylate of H2B's Glu-32 (interaction with the N-terminal helix dipole) were maintained in the truncated variants. After the initiating methionine, the sequences of ΔN-H2A and ΔN-H2B genes begin with the codons for residues Thr-16 and Glu-32, respectively. The ΔN-H2A construct includes an N-terminal turn of helix that proceeds the canonical histone fold motif. The ΔN-H2A and ΔN-H2B variants used in this study have N-terminal truncations that are larger than the common cleavages seen in histones trypsinized in the context of the core nucleosome, at residues 12 and 23 of H2A and H2B, respectively (*19*).

Spectral Properties of the H2A−H2B Variants. The N-terminal truncations used in this study do not remove any of the 3 and 5 Tyr residues of H2A and H2B, respectively. Therefore, not surprisingly, there is little difference in the intrinsic Tyr fluorescence between the WT and truncated H2A−H2B variants (data not shown).

However, removal of the N-terminal tails does affect the far-UV CD spectra of the H2A−H2B variants, which is indicative of effects on the secondary structural content of the variant dimers. In Figure 2, the CD spectra are presented in two ways: (A) the ellipticity values at the same dimer concentrations for all four proteins, reflecting the amount of secondary structure present in each dimer, irrespective of number of residues; and (B) the ellipticity values are normalized on a per residue basis (mean residue ellipticity),

[1] Abbreviations: CD, circular dichroism; C_M, the urea concentration at which the apparent fraction of unfolded monomer constitutes 50% of the population; ΔN-H2A, N-terminal tail truncation of the H2A, removing residues 2 through 15; ΔN-H2B, N-terminal tail truncation of the H2B, removing residues 2−31; $\Delta G°(H_2O)$, the free energy of unfolding in the absence of denaturant; F_{app}, apparent fraction of unfolded monomer; FL, fluorescence; KPi, potassium phosphate, pH 7.2; *m* value, parameter describing the sensitivity of the unfolding transition to the [Urea]; MRE, mean residue ellipticity; std. dev., standard deviation; WT, wild-type, full-length H2A and/or H2B.

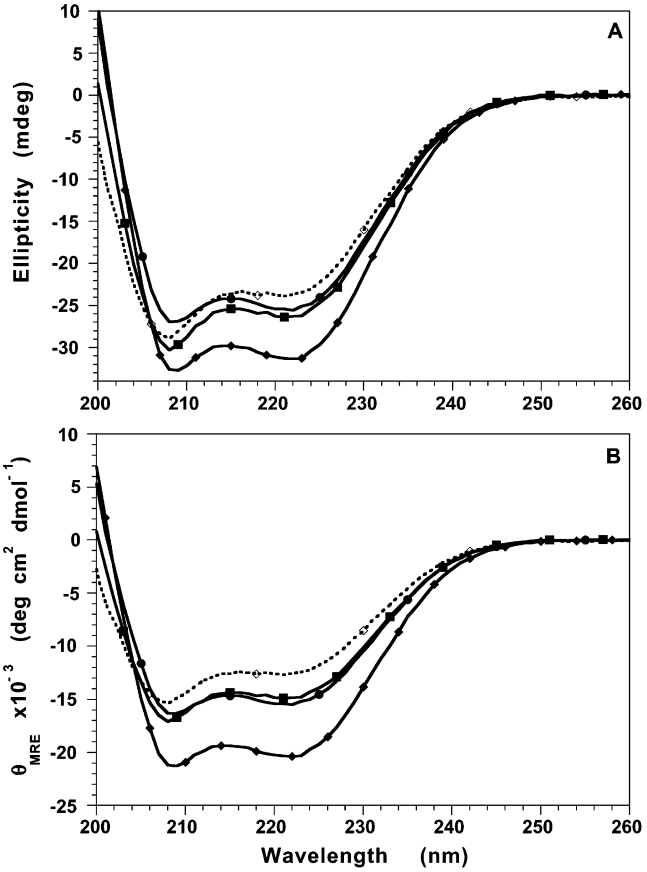

FIGURE 2: Far-UV CD spectra of WT and truncated H2A−H2B dimers. For both panels: WT H2A−H2B, ◇, dotted line; ΔN-H2A/WT-H2B, ■; WT-H2A/ΔN-H2B, ●; ΔN-H2A/ΔN-H2B, ◆. (A) Spectra at 5 μM dimer and not corrected for differences in the number of the residues in the variant dimers. (B) Spectra in units of mean residue ellipticity (MRE) and thus normalized for number of residues in the polypeptide chains. Conditions: 20 mM potassium phosphate, 0.1 mM EDTA, pH 7.2, 25 °C.

Table 1: Analysis of the CD Spectra of WT and N-terminal Truncated H2A−H2B Variants

parameter	WT H2A WT H2B	ΔN-H2A WT H2B	WT H2A ΔN-H2B	ΔN-H2A ΔN-H2B
MRE × 10^{-3}, 220 nm (deg cm^2 dmol^{-1})[a]	−12.6	−14.8	−15.4	−20.2
# residues in dimer[b]	251	237	221	207
% α-helix[c]	40/39	48/48	50/49	58/63
% α-helix expected[d]	−	42	45	48
# residues helical by CD[e]	100	114	110	120/130

[a] CD signal, corrected to mean residue ellipticity, for the H2A−H2B variants are shown in Figure 2B. [b]The number of residues assumes the removal of the N-terminal Met, as seen for the WT histones (*12*). [c]The % α-helix for each H2A−H2B variant was calculated from the spectra using two methods Selcon3 and Contin/ll; the results are given as the first and second values, respectively. [d]Amount of helix expected, relative to the WT H2A−H2B dimer with 40% helix, if the N-terminal deleted regions contained no helical structure and their removal did not induce formation of helical structure. [e]% helix determined from deconvolution of the CD spectra multiplied by number of residues in the dimer.

reflecting the fewer residues present in the ΔN-H2A and ΔN-H2B containing variants. The percentages of α-helix were calculated using the methods of Selcon3 and Continell to analyze the entire spectra. The two methods gave similar results (Table 1). Similar results were also obtained using equations that employ only the mean residue ellipticity at 220 and 222 nm (data not shown) and have been previously applied to the histone octamer (*20*). The percent helix calculated for the WT dimer, ∼40%, is reasonably close to that observed in the X-ray structure of the nucleosome, 48%. The X-ray structure includes the H3−H4 tetramer and DNA, which may stabilize additional helical structure compared to the dimer in isolation.

The spectra in Figure 2A clearly demonstrate that the three N-terminal truncations of the H2A−H2B dimer increase the amount of helix on a per dimer basis. This finding is not surprising, as the X-ray crystal structure of the nucleosome (*7*) suggested that the conformations of the tails, to the extent that the residues can be observed, are largely unstructured chains extending away from the helical regions of the dimer (Figure 1). Normalizing the CD spectra to mean residue ellipticity (Figure 2B) corrects for the different number of residues in the WT and truncated dimers. The percent helix increases more for the truncated H2A−H2B variants than expected for the removal of the unstructured regions of the N-terminal tails (Table 1). For example, if the 44 N-terminal residues deleted in ΔN-H2A/ΔN-H2B are unstructured, then the percent helix of this variant should be ∼100 residues of 207 residues, or 48%, relative to the 40% observed for the WT. The far-UV CD spectrum predicts 58−63% helix for the tail-less variant. Smaller differences between expected and those predicted from the CD spectra are observed for the single-tail variants.

Stability of the H2A−H2B Variants in 200 mM KCl. The equilibrium stability of the H2A−H2B variants were determined under conditions of physiological ionic strength ($\mu \approx 0.2$ M). The urea-induced equilibrium unfolding responses of the H2A−H2B heterodimer variants were monitored by far-UV CD and intrinsic Tyr fluorescence. Like the WT H2A−H2B heterodimer (Gloss and Placek, preceding paper), the unfolding of the truncated variants was highly reversible with no hysteresis. For the three truncated dimer variants, reversibility was assessed by comparing the CD and FL spectra of matched, individual samples at several urea concentrations over a range which spanned the unfolding transition. The matched samples were prepared individually from either an unfolded or a folded protein stock. The spectral intensities of samples derived from unfolding and refolding the two protein stocks agreed to within 90−95%. Therefore, removal of the N-terminal tails did not affect the reversibility of the urea-induced equilibrium unfolding.

For all three truncated H2A−H2B dimers, unfolding transitions were collected as a function of dimer concentration: nine data sets for ΔN-H2A/WT H2B from 1 to 30 μM dimer; nine data sets for WT H2A/ΔN-H2B from 1−20 μM dimer; and six data sets for ΔN-H2A/ΔN-H2B from 1−10 μM dimer. Most of the data sets are shown as F_{app} curves in Figure 3 (some duplicate data sets were omitted for clarity). Indicative of two-state equilibrium processes, with no populated intermediates, (1) the far-UV CD and FL transitions for a given dimer concentration, were superimposable, and (2) the data as a function of [dimer] were well-described by global fitting to a two-state dimeric model (Figure 3).

In the data analyses, the $\Delta G°(H_2O)$ and m values were treated as global parameters describing all of the data sets for a given heterodimer; the pre- and post-transition baselines were treated as local fitting parameters. The resulting fits of the data are illustrated by the solid lines in Figure 3. To

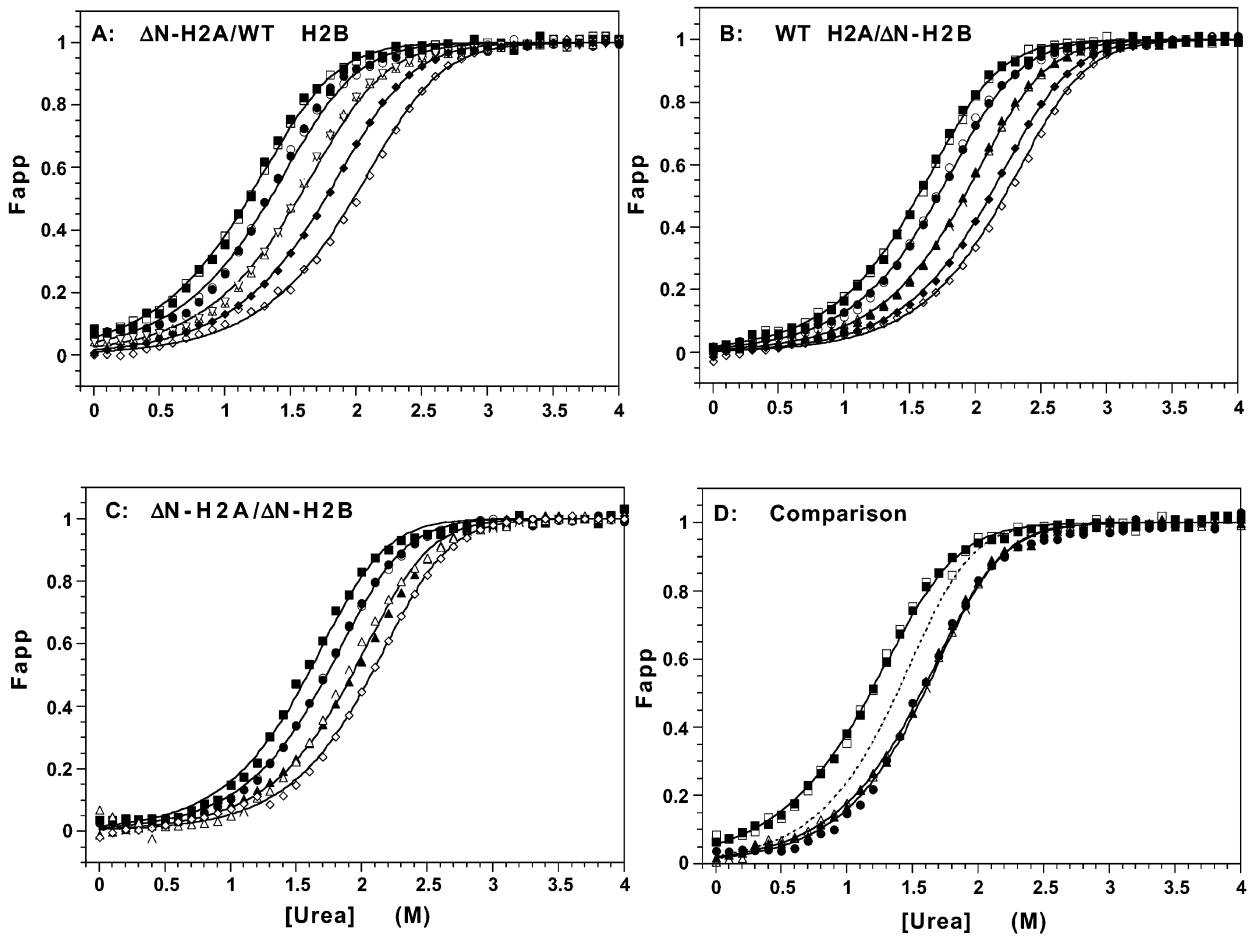

FIGURE 3: Representative urea-induced equilibrium denaturation transitions at several dimer concentrations for the N-terminal-truncated H2A−H2B variants. Data for the CD and FL titrations were collected to urea concentrations higher than shown (generally 5−6 M), but the region of the unfolding transition has been expanded for clarity. The lines represent the global fits of multiple equilibrium data sets for each dimer variant. (A) ΔN-H2A/WT-H2B at the following: 1 μM CD, ■, and FL, □; 2 μM CD, ●, and FL, ○; 5 μM FL, Δ and ∇; 12 μM FL, ◆; 30 μM FL, ◇. (B) WT-H2A/ΔN-H2B at the following: 1 μM CD, ■, and FL, □; 2 μM CD, ●, and FL, ○; 5 μM CD, ▲, and FL, Δ; 12 μM FL, ◆; 20 μM FL, ◇. (C) ΔN-H2A/ΔN-H2B at the following: 1 μM CD, ■; 2 μM CD, ●, and FL, ○; 5 μM CD, ▲, and FL, Δ; 10 μM FL, ◆. (D) Overlay of the three H2A−H2B variants at 1 μM dimer: ΔN-H2A/WT-H2B, squares; WT-H2A/ΔN-H2B, triangles; ΔN-H2A/ΔN-H2B, circles. For comparison, the fit of the full-length H2A−H2B dimer (Gloss and Placek, preceding manuscript) is represented by the dotted line. The size of the data points are equal to or larger than the error in the measurement. Conditions: 20 mM potassium phosphate, 0.1 mM EDTA, pH 7.2, 25 °C.

improve the certainty of the determination of the *m* value, given the short folded baselines at low dimer concentrations, a second global fit was performed on a larger number of data sets for each H2A−H2B variant that included the data described above at 200 mM KCl as a function of [dimer], as well as data sets at 5 μM dimer as a function of [KPi] and [KCl] (see below). The *m* value for each dimer was treated as a global parameter for all data sets (29, 28, and 23 titrations for ΔN-H2A/WT H2B, WT H2A/ΔN-H2B, and ΔN-H2A/ΔN-H2B, respectively). $\Delta G°(H_2O)$ values were treated as semiglobal parameters, linked between data sets collected under the same salt and buffer conditions. The fitted values from this larger global fit for $\Delta G°(H_2O)$ at 200 mM KCl and *m* values are given in Table 2 with the error estimated at one standard deviation of the variable on the error surface of the global fit. The values in Table 2 are in good agreement with the average value of local fits of the equilibrium data and less extensive global fits of subsets of data (for example, only data as a function of [dimer] or [salt]). For all three truncated dimers, the fitted *m* values are smaller than that determined for the WT heterodimer.

The removal of the H2A N-terminal tail alone has a small but significant destabilizing effect on the heterodimer, decreasing the free energy of unfolding by 1.1 to 0.7 kcal mol^{-1} relative to the full-length heterodimer, as determined from local and global fits. Truncation of the H2B tail, either alone or with the H2A tail in the double mutant, has no significant effect on the stability, as assessed by the value of $\Delta G°(H_2O)$. The stabilities of the H2A−H2B variants can also be compared by their C_M values, the midpoint of the transition, i.e., the concentration of urea at which unfolded monomers constitute 50% of the population. By this measure, the removal of the H2B tail is stabilizing, and this stabilization is not altered by the presence or absence of the H2A tail (Figure 3D, Table 2). The lack of significant change in stability for the double-truncated dimer, relative to the WT H2A/ΔN-H2B dimer, demonstrates a lack of additivity in the effects of tail removal. Nonadditivity of mutational effects is generally interpreted as evidence of an interaction between the sites that were mutated (*21*). This interaction of the N-terminal tails need not be via physical contact, but a synergistic, global effect on the electrostatics of the dimer.

Table 2: Parameters Describing the Urea Induced Equilibrium Transitions of the H2A−H2B Variants[a]

parameter	WT H2A WT H2B[b]	ΔN-H2A WT H2B	WT H2A ΔN-H2B	ΔN-H2A ΔN-H2B
$\Delta G°(H_2O)$[c] (kcal mol^{-1})	11.8 (0.3)	11.1 (0.1)	12.2 (0.1)	11.8 (0.1)
C_M (M) [c]	1.4 (0.1)	1.2 (0.1)	1.6 (0.1)	1.6 (0.1)
m value[d] (kcal mol^{-1} M^{-1})	2.9 (0.1)	2.7 (0.1)	2.8 (0.1)	2.6 (0.1)
$\Delta(\Delta G°)/\Delta C_\mu$[e] (kcal mol^{-1} M^{-1})				
KI	1.0 (0.1)	N/A	N/A	N/A
KCl	5.9 (0.3)	6.2 (0.2)	6.1 (0.3)	6.3 (0.3)
KPi	9.7 (0.3)	11.0 (0.5)	10.9 (0.3)	11.5 (0.2)

[a] Conditions: 20 mM potassium phosphate buffer, 0.1 mM EDTA, pH 7.2, 25 °C. The values in parentheses represent the error of one standard deviation from rigorous error analysis of global fits of the data. For $\Delta(\Delta G°)/\Delta C_\mu$, the standard deviation is for linear fits of the data weighted by the errors determined from the global fits that determined the $\Delta G°(H_2O)$ and *m* values. [b]Data from Gloss and Placek, preceding paper. [c]Free energy of unfolding for transitions at relatively low ionic strength, 200 mM KCl, globally fit as a function of dimer concentration, at a standard state of 1 M dimer. Data are shown in Figure 3. The C_M, urea concentration where the unfolded monomers constitute 50% of the population, is reported for transitions at 1 μM dimer (Figure 3D). [d]Determined from global fits of transitions as a function of protein concentration (Figure 3) and transitions as a function of [KPi] and [KCl]; globally fit, salt-independent values. [e]Slope of linear fit of $\Delta G°(H_2O)$ vs ionic strength. Data are shown in Figure 4. For KI, a linear fit is not applicable to describe the data.

Effect of Salts on the Stability of the H2A−H2B Variants. The effects of multiple salts on the stability of WT H2A−H2B suggested a role for electrostatic repulsion in destabilizing the dimer (Gloss and Placek, preceding paper). This electrostatic repulsion could arise from the high charge density of the N-terminal tails (~40 mol % basic residues) and/or from interaction of the basic residues in the histone fold motifs (~6 mol % excess basic residues). To address these two possibilities, the stabilities of the truncated H2A−H2B dimers were determined as a function of KPi, KCl and KI. These salts span the Hofmeister series in their respective abilities to stabilize proteins. The addition of salts, even to molar concentrations, did not alter the two-state, highly reversible unfolding of the variant heterodimers, permitting the determination of accurate thermodynamic parameters as a function of salt.

Local fits of the unfolding transitions as a function of KCl and KPi showed that the *m* values were independent of the [salt], as observed for the WT heterodimer (Gloss and Placek, preceding paper). Therefore, the data sets were globally fitted, linking the *m* value across all titrations collected for a given heterodimer as described above; thus, the *m* value was treated as a salt-independent parameter. A linear increase in $\Delta G°(H_2O)$ with increasing concentrations of KPi and KCl was observed for all three H2A−H2B variants, as shown in Figure 4. The slopes of these lines, indicative of the efficacy of the salt in stabilizing the heterodimers, $\Delta(\Delta G°)/\Delta C_\mu$, are reported in Table 2.

The effect of increasing concentrations of KI on the stability of the truncated dimer variants (Figure 4) is clearly different than that observed for the WT dimer (Gloss and Placek, preceding paper). For WT H2A−H2B, increasing concentrations of KI caused a linear increase in the $\Delta G°(H_2O)$, with a slope of 1.0 kcal mol^{-1} M^{-1}, with a salt-independent

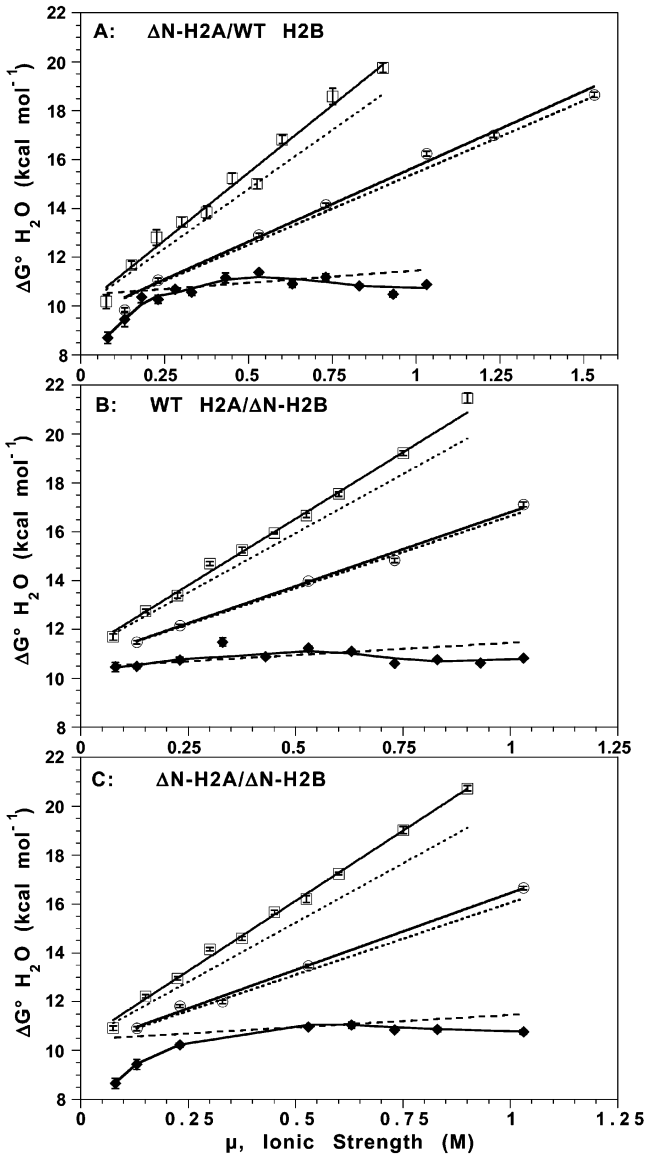

FIGURE 4: Dependence of the free energy of unfolding, $\Delta G°(H_2O)$, of the H2A−H2B variants on ionic strength with three potassium salts: KPi, □; KCl, ○; KI, ◆. (A) ΔN-H2A/WT-H2B. (B) WT-H2A/ΔN-H2B. (C) ΔN-H2A/ΔN-H2B. An error of one standard deviation on the error surface for the global fits is shown or is less than the size of the data points. The solid lines for the KPi and KCl data represent a linear fit of the data plotted as a function of ionic strength; the line for the KI data does not represent a fit but is drawn to guide the eye. For comparison, the slopes of the WT data (Gloss and Placek, preceding manuscript) are shown as dotted lines. For clarity, the slopes for the WT KCl and KPi data are normalized to the $\Delta G°(H_2O)$ in the absence of salt of the mutant data (*Y*-intercept of the linear fit), to emphasize the difference in slopes. Conditions: 5 μM dimer, at least 20 mM potassium phosphate, pH 7.2, 0.1 mM EDTA, 25 °C.

m value. For the truncated dimers, local fits of the unfolding transitions showed that the *m* values varied as a function of [KI]. For ΔN-H2A with truncated or WT H2B, the *m* values increased ~10% from 0.05 to 0.2 M KI; for WT H2A/ΔN-H2B, the *m* values decreased by ~10% over the same range of [KI]. Therefore, in the global fitting of the data, the *m* values were not treated as salt-independent parameters; only $\Delta G°(H_2O)$ was linked between the two or three unfolding transitions collected at the same [KI]. KI has no significant stabilizing effect on WT H2A/ΔN-H2B (Figure 4B) and may be slightly destabilizing at higher concentrations. For ΔN-

H2A/WT H2B and ΔN-H2A/ΔN-H2B (Figure 4A and C), KI is stabilizing up to ∼0.25 M; the slight increase in the *m* value of these dimers is consistent with a small degree of enhanced folding of the native state induced by KI. At higher KI concentrations, there is no effect or a slight destabilization. The $\Delta G°(H_2O)$ values for the three truncated variants do not increase linearly as a function of the square root of ionic strength (data not shown).

For the WT dimer, the $\Delta G°(H_2O)$ value for KI extrapolated to the absence of KI is the same, within error, for that observed in similar extrapolatations for other salts (Gloss and Placek, preceding paper). For the variant dimers, the extratrapolated $\Delta G°(H_2O)$ values to the absence of salt are similar for the KPi and KCl data, but significantly lower for the KI data, 1−2 kcal mol^{-1}. These data demonstrate that KI is destabilizing to the H2A−H2B dimer in the absence of the N-terminal tails.

DISCUSSION

Removal of the N-Terminal Tails Enhances the Helical Content of the H2A−H2B Dimer. Comparison of the far-UV CD spectra of full-length and the ΔN dimers shows that the removal of the N-terminal tails increases the ellipticity and the overall percentage of residues in helical conformation in the heterodimers (Figure 2A). Various prediction methods demonstrate that the increase in % helical content of the truncated variants is greater than expected for simply just removing unstructured, nonhelical tails (Figure 2B, Table 1). This increased helicity demonstrates that removal of the tails actually promotes the formation of helical structure in the H2A−H2B dimer and suggests that the presence of the N-terminal tails destabilizes structure in helical regions of histone proteins, at least in the absence of DNA. The effects on helicity are similar for the H2A tail and the H2B tail, which contains nearly twice the number of residues.

Effects of the N-Terminal Tails on the Stability of the H2A−H2B Dimer. Like the heterodimer of full-length H2A−H2B, the ΔN heterodimeric variants unfold under the influence of urea by a highly reversible, two-state process. Similar two-state unfolding was also observed in the thermal denaturation of the H2A−H2B histones (*11*, *22*). The lack of equilibrium intermediates demonstrates that the monomers are incapable of folding in isolation under conditions that destabilize the native heterodimer.

The values of $\Delta G°(H_2O)$ (Table 2) and C_M (Figure 3D) demonstrate that the ΔN-H2A/WT H2B dimer is destabilized relative to the full-length dimer. Therefore, the H2A N-terminal must stabilize the full-length protein. In contrast, the ΔN-H2A/ΔN-H2B and WT H2A/ΔN-H2B heterodimers have stabilities that are the same as or slightly greater than that of full-length H2A−H2B (Table 2; Figure 3D). The effects of the tail truncations in the double mutant, relative to the two single mutants, are not additive. Any destabilization resulting from truncation of the H2A N-terminal tail is mitigated in the double truncated variant; this may be the result of the enhanced helical structure in the ΔN-H2A/ΔN-H2B variant, 20−30 residues relative to the full-length dimer.

The *m* value (eq 1) describes the sensitivity of the unfolding transition to the denaturant concentration. In proteins that unfold by a two-state equilibrium reaction, this parameter correlates with the change in solvent-accessible surface area between the folded and unfolded species (*23*). The *m* value for the full-length heterodimer is larger than expected if the N-terminal tails are in an extended conformation in the native state (Gloss and Placek, preceding paper) and suggested that the N-terminal tails in the isolated, folded heterodimer adopted a collapsed, solvent-excluding structure. This interpretation predicts that removal of the N-terminal tails should decrease the *m* values observed for the ΔN truncated heterodimers. The global fits of the equilibrium unfolding data show that the truncation of the N-terminal tails decreases the observed *m* values beyond the error of the measurement. The magnitude of the decrease in the *m* value for the ΔN dimers may be attenuated by the enhanced helical structure that exist in these H2A−H2B variants (Figure 2B, Table 1).

An alternative explanation for the decreased *m* value of the ΔN H2A−H2B variants is that their unfolding transition is not a cooperative, completely two-state transition, i.e., there is an intermediate populated at equilibrium, but at such low levels that it cannot be directly detected by the methods employed. Such an equilibrium intermediate has been detected in this way for RNase H (*24*). For removal of the N-terminal tails to alter the *m* value, the tails must influence the stability of the H2A−H2B dimer and destabilize a putative equilibrium intermediate, i.e., the intermediate is more populated in the absence of the tails. Unstructured, extended N-terminal tails could only influence the stability of the rest of the protein through long distance interactions, such as electrostatic effects. Therefore, this alternative interpretation of the *m* values still suggests that electrostatic repulsion in the N-terminal tails affects the stability of the H2A−H2B dimer.

The ΔC_P is the heat capacity difference between the native and unfolded states determined from thermal denaturation experiments, such as differential scanning calorimetry. This parameter also correlates with change in solvent-accessible surface area between the native and unfolded species, like the *m* value from denaturant-induced unfolding experiments (*23*). When compared at similar solvent conditions (pH 6.0−6.5 and 25−50 mM NaCl), the full-length H2A−H2B dimer exhibited a higher ΔC_P value, 1.3−1.4 kcal K^{-1} mol^{-1}, than that of the trypsinized, tail-less dimer, 1.1 kcal K^{-1} mol^{-1} (*11*, *22*). This trend is consistent with the findings of this report on the decreased *m* values of the ΔN H2A−H2B variants.

The salt-induced stabilization of the ΔN and WT H2A−H2B variants were determined (Figure 4, Table 2). A discussion of the different stabilizing mechanisms of salts is presented in the preceding paper (Gloss and Placek). For full-length H2A−H2B, the predominant stabilizing effect of salts was via a preferential hydration/Hofmeister effect mechanism (for review, see refs *25*−*28*). However, electrostatic repulsion plays a role in destabilizing the WT heterodimer. The following discussion supports this interpretation and suggests that the electrostatic repulsion arises from residues in the N-terminal tails.

KPi is a potent stabilizer of the full-length H2A−H2B dimer, doubling the free energy of unfolding across a concentration range of 20−700 mM (Gloss and Placek, preceding paper). The efficacy of KPi to stabilize the heterodimers, $\Delta(\Delta G°)/\Delta C_\mu$ values, for the truncated variants are 1.2−1.8 kcal mol^{-1} M^{-1} greater than that exhibited by

the full-length heterodimer (Table 2). If the KPi stabilization of the H2A−H2B dimers is solely the result of a preferential hydration mechanism (*27*, *28*), removal of the N-terminal tails should have no effect on or decrease the efficacy of KPi to stabilize the truncated variants. The magnitude of stabilization by preferential hydration can be considered in terms of a thermodynamic cycle of free energies: the free energy of transfer for the native and unfolded states from water to the solution containing the excluded cosolute and free energies of unfolding in water and in the presence of the excluded cosolute (*27*, *29*). Stabilization arises from the increase in the free energy of the denatured state, relative to the native state, in the presence of the cosolute because the surfaces exposed upon denaturation enhance the preferential exclusion of the cosolute. If the solvent-accessible surface area of a region of the protein does not change upon unfolding, then that region of the protein will not contribute to stabilization by preferential hydration. The expected effects on the $\Delta(\Delta G°)/\Delta C_\mu$ values are considered below for two scenarios regarding the N-terminal tails IF preferential hydration is the only mechanism of action of KPi.

(1) The N-terminal tails are in an unfolded conformation in the native state: There will be no significant difference in hydrophobic surface area exposed to water and excluded cosolute upon protein unfolding in the presence or absence of the N-terminal tails. Therefore, removal of the tails should have no effect on stabilization by a Hofmeister ion; the $\Delta(\Delta G°)/\Delta C_\mu$ values should be the same for the WT and truncated dimers.

(2) The N-terminal tails are in a collapsed, solvent-excluding structure in the native state and undergo an unfolding reaction: (Data in this report suggests this is the case; see above discussion of the *m* value.) Additional surface is exposed to solvent upon unfolding of the WT dimer, compared to the truncated dimers. Thus, removal of the tails should decrease the amount of surface that is affected by the presence of the Hofmeister ion. Therefore, the efficacy of the ion to stabilize the protein to denaturation, $\Delta(\Delta G°)/\Delta C_\mu$, should be decreased.

The observed effect of removal of the N-terminal tails, an enhanced efficacy of KPi stabilization, is not consistent with stabilization solely by preferential hydration or the Hofmeister effect. The results in Table 2 can be explained by stabilization of the full-length H2A−H2B dimer by both preferential hydration and screening of electrostatic repulsion that arises from the basic residues in the N-terminal tails.

Favorable interactions between protein side-chains and a preferentially excluded cosolute such as KPi will attenuate the stabilization by a preferential hydration mechanism (*29*, *30*). If the regions that interact favorably with the cosolute are removed, then the efficacy of the cosolute to stabilize the protein by exclusion from the surface of the protein and promoting preferential hydration should be enhanced. The greater values of $\Delta(\Delta G°)/\Delta C_\mu$ for the truncated H2A−H2B dimers, relative to WT, demonstrate that KPi interacts with these tails. Two related types of electrostatic interactions could be at work: ion binding or screening of electrostatic repulsion from the high positive charge density of the side-chains. If phosphate anions bind the tails, the affinity must be very low. The apparent dissociation constant must exceed 500 mM, as the plots of $\Delta G°(H_2O)$ (Figure 4) and C_M (data not shown) as a function of [KPi] show no curvature that would indicate an approach to saturation of the binding site(s), as seen for phosphate binding stabilizing the ribonuclease P protein (*31*).

An estimate of the stabilization from screening electrostatic repulsion was made by extrapolating the $\Delta G°(H_2O)$ values to 0 M, to estimate the stability in the absence of preferential hydration. Relative to WT H2A−H2B, the stabilities of ΔN-H2A/WT H2B, WT H2A/ΔN-H2B, and ΔN-H2A/ΔN-H2B are increased by 0.8, 2.0, and 1.3 kcal mol^{-1} (with errors of 0.06−0.1 kcal mol^{-1}), respectively. Similar, but slightly smaller estimates, were obtained from the KCl data sets. These differences in free energy suggest that electrostatic repulsion decreases the stability of the dimers by ∼7−15% at a standard state of 1 M dimer. The value of $\Delta(\Delta G°)/\Delta C_\mu$ is independent of dimer concentration. At more physiological dimer concentrations, such as those employed in these experiments, the contribution of electrostatic interactions is higher. For example, at 10 μM dimer, the contribution of electrostatic repulsion decreases the stability of the dimers by 20−40%. As shown previously by thermal denaturation (*11*), the tails are not the major contributor to the stability of the H2A−H2B dimer. However, electrostatic repulsion from the N-terminal tails plays a significant role in the stability of the dimer.

A similar trend of enhanced efficacy is seen for the KCl stabilization of the ΔN H2A−H2B dimers relative to the full-length dimer. However, the effect is smaller, with $\Delta(\Delta G°)/\Delta C_\mu$ values only ∼0.3 kcal mol^{-1} M^{-1} greater for the truncated dimers relative to the full-length dimer (Table 2). KCl is lower on the Hofmeister scale than KPi. Accordingly, KCl should be less preferentially excluded from the surface of proteins than is KPi. Therefore, the attenuation of stabilization by a preferential hydration mechanism should be less for KCl than for KPi.

KI is generally considered to be a mild protein denaturant. However, as a salt, KI can stabilize a protein by screening electrostatic repulsion. This favorable effect is observed in the mild KI stabilization of full-length H2A−H2B, resulting in a linear increase in $\Delta G°(H_2O)$ of 1 kcal mol^{-1} M^{-1} (Gloss and Placek, preceding paper). The data for the H2A−H2B variants suggests that the stabilization of WT by KI is the result of screening electrostatic repulsion primarily within the N-terminal tails. Therefore, when the tails are truncated, the stabilizing effects of increasing [KI] are largely mitigated, and destabilization is apparent when $\Delta G°(H_2O)$ values are extrapolated to the absence of salt. However, there appears to be some stabilization by KI from interactions with the histone fold motif, indicated by the effects on the ΔN-H2A containing dimers (Figures 4A and C). However, this stabilization is largely complete by ∼0.2 M KI, whereas KI continues to stabilize full-length H2A−H2B up to 0.8 M KI.

Comparison to Previous Reports on the Stability of the H2A−H2B Dimer. Thermal denaturation, using differential scanning calorimetry and far-UV CD, of WT and trypsinized H2A−H2B dimers (removing the N termini of both histones and the C-terminal tail of H2A) have been reported previously (*11*, *22*). Thermal denaturation, in general, may have an advantage over chemical denaturants in studies that address the role of cosolutes on the stability of proteins. Over the concentration range employed in an equilibrium urea denaturation experiment, the concentration of cosolutes is

drastically changed. Therefore, with a background of 0−7 M urea, the effects of submolar salt concentrations may not be as dramatic as in a thermal denaturation experiment where the concentrations of cosolutes are not varied across the unfolding transition. However, in the case of the H2A−H2B histones, thermal denaturation has a strong disadvantage in that the unfolding is less reversible and is hampered by aggregation at higher temperatures (*11, 22*); this aggregation is exacerbated by increased ionic strength and/or removal of the histone tails—precisely the alterations to the system that are of interest in this report. The high reversibility of the urea denaturation of the H2A−H2B dimers was not affected by increased ionic strength or removal of the N-terminal tails. This advantage of urea denaturation permits the determination of more accurate and precise thermodynamic parameters to allow the elucidation of the subtle effects of salts and N-terminal tail deletions.

Thermal denaturation studies comparing full-length and trypsinized H2A−H2B dimers showed that the truncated dimer is slightly more stable below 20 mM NaCl, as evidenced by a slightly higher T_M, the midpoint of the unfolding transition (*11*). At higher NaCl concentrations, the full-length dimer was slightly more stable. The authors suggested that the tails may acquire a partially ordered conformation at higher ionic strengths that contributed minor stabilization to the full-length dimer. The results of this paper show that the H2A tail is stabilizing, but that the H2B tail is slightly destabilizing. Urea denaturation results support the conclusion from the thermal denaturation data that the histone tails have a relatively small effect on the stability of the heterodimer, and that the structured domains of the histones play the central role in the thermodynamics of histone stability. However, the effects of electrostatic repulsion in the N-terminal tails, as indicated by the results of this paper, may have an important impact on nucleosome dynamics (see below).

The mechanism of stabilization of the H2A−H2B dimer by NaCl was not addressed in the thermal denaturation of the full-length (*22*) or trypsinized (*11*) dimers. The T_M values for the full-length and trypsinized dimers do not increase linearly with [NaCl] (Figure 2b of ref *11*). If the T_M data are plotted as a function of the square root of [NaCl] (data not shown), to examine electrostatic components of the stabilization, the full-length H2A−H2B displays a biphasic increase in T_M with increasing [NaCl]. From 0.01 to 0.05 M NaCl, the T_M is very sensitive to [NaCl]. From 0.1 to 1.0 M NaCl, the linear slope of T_M with increasing [NaCl] is much shallower. The increase in the T_M values of the trypsinized H2A−H2B with increasing [NaCl] is a single linear response, with a slope similar to the shallower transition observed for the full-length dimer data. The thermal denaturation data suggest that (1) electrostatic repulsion, screened by increasing concentrations of NaCl, destabilizes the full-length dimer, (2) the repulsion arises from two regions of the protein, and (3) the tail regions removed by the action of trypsin are responsible for the most sensitive region observed in the full-length dimer. This interpretation of the thermal denaturation data is consistent with the findings of this report based on urea denaturation data.

Conclusions and Implications for Function of the H2A−H2B Dimer in the Nucleosome. The data in this report support four conclusions regarding the N-terminal tails of the H2A and H2B monomers of the histone heterodimer. (1) The removal of the N-terminal tails of the H2A and H2B dimer enhances the helical content of the heterodimer (Figure 2; Table 1). (2) Removal of the H2A N-terminal tail destabilizes the ΔN-H2A/WT H2B dimer; removal of the H2B tail, alone or in the absence of the H2A tail, slightly stabilizes the heterodimers (Figure 3, Table 2). The stability effects of the single tail truncations are not additive in the effects on the ΔN-H2A/ΔN-H2B variant. (3) The decreased *m* values of the truncated heterodimers (Table 2) are consistent with the N-terminal tails adopting collapsed, solvent-excluding structures, unlike the extended conformations seen in the X-ray structures of the nucleosome (*7*). (4) There are two mechanisms operating in the H2A−H2B stabilization by potassium salts (Figure 4, Table 2). The predominant mechanism is through the preferential hydration and the Hofmeister effect. The salts also stabilize by screening electrostatic repulsion, which arises largely from the N-terminal tails of the dimer.

These data and conclusions help elucidate biophysical features that may play an important role in the dynamics of the nucleosome. To understand the equilibria and kinetics of nucleosome folding and unfolding, the stability and structure of the isolated proteins must be taken into account (discussed in Gloss and Placek, preceding paper). During transcription (and perhaps other DNA processes in the cell such as replication and repair), there is an important equilibrium between the intact histone octamer and a partially unfolded nucleosome in which the H2A−H2B dimers are more weakly bound, and perhaps partially or completely dissociated from the nucleosome. Stabilization of the isolated H2A−H2B dimer will favor a more unfolded, dissociated state of the nucleosome. A potential mechanism to stabilize the histones is to reduce electrostatic repulsion on these highly charged oligomers. Acetylation of Lys residues and phosphorylation of adjacent Ser residues in the N-terminal tails should serve to reduce electrostatic repulsion, stabilize the H2A−H2B dimer and alter the equilibrium between an intact and partially unfolded nucleosome. The data in this and the preceding paper (Gloss and Placek) also suggest that the N-terminal tails of H2A−H2B adopt a collapsed structure in the isolated dimer. This structure should be similarly stabilized by posttranslational modifications to the tails that reduce electrostatic repulsion. Hyperacetylation has been reported to enhance helical structure in the N-terminal tail of H4 (*20*). To fully understand the equilibria involved in the folding and unfolding of the nucleosome, the presence and alteration of folded conformations in the N-terminal tails of the isolated histone oligomers should be determined and considered.

ACKNOWLEDGMENT

We dedicate this paper to the memory of our late colleague, Jeremy N.S. Evans, in appreciation for his friendship and scientific insights and guidance. Douglas D. Banks assisted in determining the molecular weight of the dimers by HPLC size-exclusion chromatography coupled to light-scattering. Helpful discussions and critical review of the manuscript by Traci Topping and Dr. Michael J. Smerdon are appreciated. The pET overexpression vectors for the wild-type histone genes were kindly provided by Drs. Karolin Luger (currently at Colorado State University) and Timothy

Richmond of the Instititute for Molecular Biology and Biophysics at the ETHZ, Zurich, Switzerland.

REFERENCES

1. Workman, J. L., and Kingston, R. E. (1998) Alteration of nucleosome structure as a mechanism of transcriptional regulation, *Annu. Rev. Biochem. 67*, 545−79.
2. Wolffe, A. P., and Guschin, D. (2000) Chromatin structural features and targets that regulate transcription, *J. Struct. Biol. 129*, 102−122.
3. Cheung, P., Allis, C. D., and Sassone-Corsi, P. (2000) Signaling to chromatin through histone modification, *Cell 103*, 263−71.
4. Strahl, B. D., and Allis, C. D. (2000) The language of covalent histone modifications, *Nature 403*, 41−5.
5. Anderson, J. D., Lowary, P. T., and Widom, J. (2001) Effects of histone acetylation on the equilibrium accessibility of nucleosomal DNA target sites, *J Mol Biol 307*, 977−85.
6. Arents, G., and Moudrianakis, E. N. (1993) Topography of the histone octamer surface: Repeating structural motifs utilized in the docking of nucleosomal DNA, *Proc. Natl. Acad. Sci. U.S.A. 90*, 10489−93.
7. Luger, K., Mader, A. W., Richmond, R. K., Sargent, D. F., and Richmond, T. J. (1997) Crystal structure of the nucleosome core particle at 2.8 A resolution, *Nature 389*, 251−60.
8. Xie, X., Kokubo, T., Cohen, S. L., Mirza, U., Hoffmann, A., Chait, B. T., Roeder, R. G., Nakatani, Y., and Burley, S. K. (1996) Structural similarity between TAFs and the heterotetrameric core of the histone octamer, *Nature 380*, 316−322.
9. Birck, C., Poch, O., Romier, C., Ruff, M., Mengus, G., Lavigne, A. C., Davidson, I., and Moras, D. (1998) Human $TAF_{II}28$ and $TAF_{II}18$ interact through a histone fold encoded by atypical evolutionary conserved motifs also found in the SPT3 family, *Cell 94*, 239−49.
10. Arents, G., Burlingame, R. W., Wang, B. C., Love, W. E., and Moudrianakis, E. N. (1991) The nucleosomal core histone octamer at 3.1 Å resolution: a tripartite protein assembly and a left-handed superhelix, *Proc. Natl. Acad. Sci. U.S.A. 88*, 10148−52.
11. Karantza, V., Freire, E., and Moudrianakis, E. N. (2001) Thermodynamic studies of the core histones: Stability of the octamer subunits is not altered by removal of their terminal domains, *Biochemistry 40*, 13114−123.
12. Luger, K., Rechsteiner, T. J., Flaus, A. J., Waye, M. M., and Richmond, T. J. (1997) Characterization of nucleosome core particles containing histone proteins made in bacteria, *J. Mol. Biol. 272*, 301−311.
13. Sang, N., Condorelli, G., De Luca, A., MacLachlan, T. K., and Giordano, A. (1996) Generation of site-directed mutagenesis by extralong, high fidelity polymerase chain reaction, *Anal. Biochem. 233*, 142−144.
14. Sreerama, N., and Woody, R. W. (2000) Estimation of protein secondary structure from circular dichroism spectra: comparison of CONTIN, SELCON, and CDSSTR methods with an expanded reference set, *Anal. Biochem. 287*, 252−60.
15. Johnson, W. C. (1999) Analyzing protein circular dichroism spectra for accurate secondary structures, *Proteins 35*, 307−12.
16. Sreerama, N., and Woody, R. W. (1994) Protein secondary structure from circular dichroism spectroscopy. Combining variable selection principle and cluster analysis with neural network, ridge regression and self-consistent methods, *J. Mol. Biol. 242*, 497−507.
17. Provencher, S. W., and Glockner, J. (1981) Estimation of globular protein secondary structure from circular dichroism, *Biochemistry 20*, 33−7.
18. Sreerama, N., Venyaminov, S. Y., and Woody, R. W. (1999) Estimation of the number of alpha-helical and beta-strand segments in proteins using circular dichroism spectroscopy, *Protein Sci. 8*, 370−80.
19. Hansen, J. C., Tse, C., and Wolffe, A. P. (1998) Structure and function of the core histone N-termini: More than meest the eye, *Biochemistry 37*, 17637−17641.
20. Wang, X., Moore, S. C., Laszckzak, M., and Ausió, J. (2000) Acetylation increases the α-helical content of the histone tails of the nucleosome, *J. Biol. Chem. 275*, 35013−35020.
21. Wells, J. A. (1990) Additivity of mutational effects in proteins. *Biochemistry 29*, 8509−17.
22. Karantza, V., Baxevanis, A. D., Freire, E., and Moudrianakis, E. N. (1995) Thermodynamic studies of the core histones: Ionic strength and pH dependence of H2A−H2B dimer stability, *Biochemistry 34*, 5988−96.
23. Myers, J. K., Pace, C. N., and Scholtz, J. M. (1995) Denaturant *m* values and heat capacity changes: Relation to changes in accessble surface areas of protein folding, *Protein Sci. 4*, 2138−2148.
24. Spudich, G., and Marqusee, S. (2000) A change in the apparent *m* value reveals a populated intermediate under equilibrium conditions in *Escherichia coli* ribonuclease HI, *Biochemistry 39*, 11677−83.
25. Baldwin, R. L. (1996) How Hofmeister ion interactions affect protein stability, *Biophys. J. 71*, 2056−63.
26. Record, M. T., Jr., Zhang, W., and Anderson, C. F. (1998) Analysis of effects of salts and uncharged solutes on protein and nucleic acid equilibria and processes: A practical guide to recognizing and interpreting polyelectrolyte effects, Hofmeister effects and osmotic effects of salts, *Adv. Protein Chem. 51*, 282−355.
27. Timasheff, S. N. (1993) The control of protein stability and association by weak interactions with water: How do solvents affect these processes? *Annu. Rev. Biophys. Biomol. Struct. 22*, 67−97.
28. Timasheff, S. N. (1998) Control of protein stability and reactions by weakly interacting cosolvents: The simplicity of the complicated, *Adv. Protein Chem. 51*.
29. Bolen, D. W., and Baskakov, I. V. (2001) The osmophobic effect: Natural selection of a thermodynamic force in protein folding, *J. Mol. Biol. 310*, 955−963.
30. Saunders, A. J., Davis-Searles, P. R., Allen, D. L., Pielak, G. J., and Erie, D. A. (2000) Osmolyte-induced changes in protein conformational equilibria, *Biopolymers 53*, 293−307.
31. Henkels, C. H., Kurz, J. C., Fierke, C. A., and Oas, T. G. (2001) Linked folding and anion binding of the *Bacillus subtilis* ribonuclease P protein, *Biochemistry 40*, 2777−89.
32. Kraulis, P. J. (1991) MOLSCRIPT: a program to produce both detailed and schematic plots of protein structures, *J. Appl. Crystallogr. 24*, 946−950.

BI026283K